Genomic Psychiatry

Genomic Press Genomic Psychiatry Advancing science from genes to society

OPEN

PERSPECTIVE

Illuminating synucleinopathies: Advances in α -synuclein PET tracer development for in vivo neuroimaging

Yingfang He¹, Liyun Qin², Qing Ye², and Fang Xie³

Abnormal α -synuclein aggregation is a pathological hallmark of Parkinson's disease, multiple system atrophy, and dementia with Lewy bodies. A suitable radiotracer that can noninvasively map synucleinopathies through positron emission tomography (PET) will lead to breakthroughs in early diagnosis, monitoring disease progression, and evaluating treatment responses. However, the development of PET tracers for α -synuclein is lagging due to several challenges. In this perspective, we provide a brief review of the advancements in PET tracers targeting α -synuclein and summarize recent clinical studies aimed at mapping synucleinopathies in neurodegenerative patients using these PET tracers.

Genomic Psychiatry July 2025;1(4):34-39; doi: https://doi.org/10.61373/gp025p.0032

Keywords: α-synuclein, clinical studies, PET neuroimaging, radiotracer development, structure optimization

Aggregation of α -synuclein is found in Lewy bodies (LBs) and Lewy neurites (LNs), which are the pathological hallmarks of Parkinson's disease (PD) and related disorders known as synucleinopathies (1, 2). However, the regional distribution, conformation, and seeding capacity of synucleinopathies are heterogeneous among the diseases. In PD, neuronal inclusions of LBs and LNs first emerge in the brainstem, spreading through the midbrain/substantia nigra to the medial temporal cortex, and through the mesocortex to the neocortex (3). In comparison, the cellular pathology of dementia with Lewy bodies (DLB) is characterized by glial cytoplasmic inclusions found in oligodendrocytes, which are particularly prominent in the white matter of the brainstem and cerebellum (4). SNCA gene located in chromosome region 4g21-4g23 is responsible for encoding the α -synuclein protein in humans. The protein consists of three distinct regions: (1) an amphipathic domain (residues 1-60) that contains apolipoprotein lipid-binding motifs, which are predicted to form amphiphilic helices, thereby conferring a propensity to adopt α -helical structures upon membrane binding, (2) a non-amyloid β -component (NAC) (residues 61–95), which is crucial for potential β -sheet aggregation, and (3) an acidic domain that is highly negatively charged and prone to being unstructured (Figure 1) (5-7). In 1997, Polymeropoulos et al. identified the first missense variant in SNCA, leading to an A53T amino acid change and, as a result, a prolonged β structure that is prone to aggregation (8). Since then, several other point mutations in SNCA have been reported, including E46K (9), G51D (10), E83Q (11), and V15A (12) depicted in Figure 1. Nevertheless, a common mechanism by which SNCA point mutations might result in synucleinopathies has yet to be discovered, indicating that the diverse genetic architecture may influence clinical and pathological presentations through distinct signaling pathways (13). In addition, a diverse set of variants contributing to mitochondrial and mitophagy function, lysosomal and trafficking pathways, and so on, are inversely or directly correlated with the level of synucleinopathies, such as LRRK2, PARK7 (also known as DJ-1), PRKN (also known as PARK2), and PINK1 (14).

Molecular probes with an appropriate affinity, high selectivity, and specificity in vivo for α -synuclein will be useful in the understanding and monitoring of synucleinopathy-related diseases using positron emission tomography (PET). This could be exemplified by radioligands targeting tauopathies, which provide PET-based Braak staging as an

effective method to differentiate between phases of the AD continuum (15). Our recent studies have shown that synaptic loss in the brain measured by [18F]SynVesT-1, a 18F-radiolabeling radiotracer that targets synaptic vesicle glycoprotein 2A, correlates with clinical, fluid, and imaging biomarkers of neurodegeneration (16, 17). This finding supports the use of PET imaging as a valuable tool for assessing interconnected pathologic processes, including pathologic structures, neuroinflammation, and synaptic dysfunction. Furthermore, in vivo PET quantification can expedite drug discovery and development by providing valuable information on accessing target occupancy and monitoring treatment feedback. A β targeting monoclonal antibodies such as aducanumab and lecanemab gained accelerated FDA approval based on the reductions of amyloid- β $(A\beta)$ PET signals in clinical trials. Undoubtedly, there is much interest to develop radiotracer for mapping synucleinopathies in the brain regions. In this perspective, we aimed to briefly review the development of PET tracers targeting α -synuclein (Figures 2 and 3) and highlight recent advances that may illuminate the path for future development.

Thioflavin-T derivative [11C]Pittsburgh compound-B ([11C]PIB) and benzoxazole [18F]BF227 were first investigated as non-selective probes for $\beta\text{-sheet}$ structures of $\alpha\text{-synuclein}$ aggregates. Using $\alpha\text{-synuclein}$ or $A\beta_{1-42}$ fibrils, [18 F]BF227 showed high binding affinity to β -sheet structures of both species with two classes of binding sites on $A\beta_{1-42}$ fibrils (dissociation constants $K_{d1} = 1.31$ and $K_{d2} = 80$ nM, respectively) and one class of binding sites on α -synuclein fibrils ($K_d = 9.63$ nM) (18). Fluorescent BF227 staining of the substantia nigra from patients with PD showed also colocalization with immunohistochemistry staining using an α -synuclein-targeting antibody. However, no binding of [18 F]BF227 was detected in pure DLBs homogenates in the absence of A β plaques. This observation suggests that the structure of recombinant fibrils may not accurately reflect the structure of fibrils existed in brain homogenates, particularly due to the potential impact of posttranslational modifications and protein interactions on the conformation of β -sheet structures and the accessibility of binding sites in vivo. Bagchi and Yu et al. subsequently demonstrated that the phenothiazine analog [1251]SIL23 bound to a site identified on recombinant α -synuclein fibrils, as well as to fibrillar α -synuclein in LBs and LNs found in the brains of patients with PD (19). The density of corresponding binding site was proven to be sufficiently high to be detected by PET imaging using high affinity

¹Institute of Radiation Medicine, Fudan University, Shanghai 200032, China; ²Department of Neurology, Longhua Hospital, Shanghai University of Traditional Chinese Medicine, Shanghai 200032, China; ³Department of Nuclear Medicine & PET Center, Huashan Hospital, Fudan University, Shanghai 200230, China

Corresponding Authors: Fang Xie, Department of Nuclear Medicine & PET Center, Huashan Hospital, Fudan University, Shanghai 200230, China. E-mail: fangxie@fudan.edu.cn



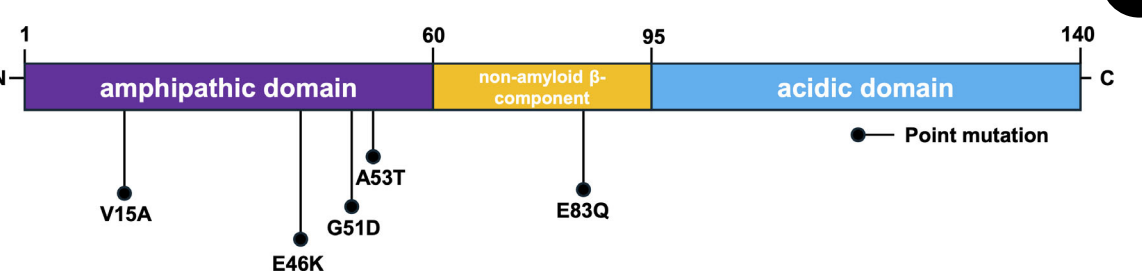


Figure 1. Schematic of α -synuclein domains.

 tracer has been used in human studies H_3C ¹¹CH₃ [125|]SIL23 • [¹¹C]PIB • [18F]BF227 NO_2 $^{11}\mathrm{CH}_3$ [11C]anle253b [¹¹C]MODAG-[¹⁸F]46a 001 ¹¹CH₃ [¹⁸F]FS3-1 [11C]APT-13 $[^{18}F]MFSB: X = O$ $[^{18}F]PFSB: X = CH_2$ [18F]F-0502B [18F]SPAL-T-06: X = N

Figure 2. Chemical structures of α -synuclein PET tracers.

• [¹⁸F]C05-05: X = C

[¹⁸F]ACI-12589



Cpd.	х	A	a-syn <i>K</i> _i (nM)	Αβ Κ _i (nM)
4f	Н	-{	21.9 ± 9.7	≥ 760
4i ^a	н		6.1 ± 2.1	N. A ^b
4m	Н	ZZN N	8.7 ± 0.6	>1000
40	N		4.9 ± 0.4	43.1 ± 3.8
4p	N	N	44.1 ± 32.0	N. A
B S N S N S N S N S N S N S N S N S N S			$N \longrightarrow N \longrightarrow N \longrightarrow 18F$ $[^{18}F]FITA-2$	

Figure 3. (A) Structure-affinity relationship of **4i** and its derivatives (32). ^aThe compound was labeled with carbon-**11** and evaluated as a PET tracer targeting α -synuclein. ^bN.A stands for not active (no displacement at 1000 nM). (B) Chemical structures of [18 F] FITA-2.

radioligands. However, not yet a tricyclic structure based on SIL23 has been reported for imaging synucleinopathies in patients. [18 F]46a reported by Chu *et al.* was optimized from selective fluorescent dyes and displayed good selectivity on α -synuclein fibrils (20). The high lipophilicity and potential reduction of the nitro group in the structure were believed to contribute to a high level of nonspecific binding in vivo, hindering its application as a suitable PET probe for neuroimaging. Inhibition pathological aggregation of prion protein and α -synuclein using diphenylpyrazole led to the discovery of [11 C]anle253b, from which [11 C]MODAG-001 was developed (21, 22). In dynamic PET imaging of normal mice, [11 C]MODAG-001 demonstrated good brain penetration; however, several radiometabolites were identified in the brain homogenates at 5 min postinjection. Further *in vitro* autoradiography studies showed

no significant binding on brain sections from patients with Lewy body dementia using $[^3H]\text{MODAG-001}.$ Like $[^{18}F]\text{46a}$, its high log\$D\$ value was proposed as the reason for the low signal-to-noise ratio in human brain tissue with synuclein pathology. Arylpyrazolethiazole derivative $[^{11}C]\text{APT-13}$ was recently reported to have a \$K_i\$ value of 27.8 \pm 9.7 nM and a 3.3-fold selectivity over \$A_{\beta}\$. In preliminary studies, it exhibited high initial brain penetration in healthy mouse brains and emerged as a lead for further development (23). Diarybisthiazole derivative $[^{18}F]\text{FS3-1}$ showed promising sensitivity in a rat model overexpressing human E46K-mutated \$\alpha\$-synuclein (24).

Meanwhile, numerous structures containing polyphenols such as gallic acid and flavonoids such as quercetin have been found to have good inhibitory effect on α -synuclein aggregation (25, 26). It's hypothesized



that phenol or catechol group promotes the interaction with α -synucleincontaining species. Accordingly, the dimethylamino group on BF227 may be accountable for its affinity toward A β fibrils, sabotaging its specificity. A novel PET tracer targeting α -synuclein ([18 F]F-0502B, Figure 2) has recently been reported (27). It is structurally similar to $[^{18}\mathrm{F}]\mathrm{BF227}$ but features a free phenol group, with molar activities ranging from 18.5 to 37 GBq/µmol. Using saturation binding assays, [18F]F-0502B exhibited $K_{\rm d}$ values of 3.68, 107.8, and 151.2 nM in brain homogenates from PD, Alzheimer's disease (AD) with Aβ fibrils and AD with tau fibrils, respectively, demonstrating its specific interactions with α -synuclein fibrils. In healthy non-human primates, [18F]F-0502B showed an initial brain uptake with a standardized uptake value (SUV) below 1.5 and fast washout within 5 min postinjection. The tracer was further investigated in nonhuman primate models of PD with nigrostriatal degeneration induced by intracranial injection of adeno-associated virus encoding A53T mutant human α -synuclein (AAV-A53T- α -Syn) or preformed fibrils of α -synuclein. PET images averaged from 30 to 60 min postinjection of [18F]F-0502B showed a higher radioactivity accumulation in the striatal regions of PD models compared with the control group. Further investigations, including radiometabolite analysis, kinetic modeling, and human translation, are warranted to see whether [18F]F-0502B could serve as a useful tracer for imaging α -synuclein aggregates in living patients. Notably, Maurer et al. disclosed the development of a library of 2-styrylbenzothiazoles in 2023 (28). Using human recombinant α -synuclein fibrils and [3 H]PIB, less lipophilic analog MFSB also exhibited enhanced affinity to α -synuclein aggregates ($K_i = 10.3 \pm 4.7$ nM) compared with that of PFSB. PET imaging demonstrated significant brain penetration of [18F]MFSB, with a SUV of 1.79 in healthy wild-type mice. However, the slow washout of [18F]MFSB from the brain, along with increased radioactivity accumulation in white matter-rich areas such as the midbrain and brainstem, indicates a high degree of nonspecific binding in vivo.

[18F]SPAL-T06 with an (E)-hex-2-en-4-yne linker in the backbone structure was reported by Higuchi et al. (29). The affinity of [18F]SPAL-T06 was determined to be 2.49 nM using putamen homogenates of patients with multiple system atrophy (MSA) with predominant parkinsonism. It successfully visualized the synucleinopathies in patients with MSA without A β deposition. However, its rapid metabolism and, consequently, insufficient intact radioligand in the bloodstream preclude its ability to capture α -synucleinopathies in cases of PD and DLB with low target abundance. The same group further developed [18F]C05-05 to overcome the rapid clearance issue of [18F]SPAL-T06 (30). In in vitro autoradiography, [18 F]CO5-05 showed specific accumulation in the amyodala from a patient with DLB and substantia nigra from a patient with PD with dementia. The concentrations of this tracer to induce 50% homologous inhibition were determined to be 1.5 and 1.7 nM in DLB and MSA homogenates, respectively. Ten patients meeting clinical diagnostic criteria for PD or DLB, and eight healthy controls were included for an exploratory clinical PET study of [18F]C05-05. The study focused on the synucleinopathies in the midbrain, as the midbrain substantia nigra is a common area affected by Lewy pathologies in "body-first" and "brain-first" subtypes of PD and DLB at a clinical stage. Using the deep white matter as the reference region, subjects in PD/DLB group showed significantly higher ratios of SUV_{midbrain}/SUV_{reference region}, which is well correlated with the degree of motor impairments assessed by Movement Disorder Society revised Unified Parkinson's Disease Rating Scale part III scores. Although patients with AD pathologies were pre-excluded, this study provided the first essential evidence on the capability of PET probe for imaging α synuclein pathologies in humans. However, it is important to note that both [18F]SPAL-T06 and [18F]C05-05 interact with the groove-like binding pocket in the β -sheet structure of α -synuclein fibril cores. This binding characteristic complicates the achievement of high selectivity over tau pathology, due to the significant resemblance of cross- β structures. Consequently, the accumulation of radioactivity from these tracers in vivo will be confounded by the presence of tau aggregations. Meanwhile, the increased nonspecific binding of [18F]C05-05 to myelin components may potentially elevate background noise in other regions with high white matter fractions. Further studies in a relatively large cohort are warranted to investigate whether the aforementioned factors have a profound

impact on its clinical value regarding disease progression and companion diagnosis.

[18F]ACI-12589, developed by the biotech company AC Immune, was recently published and demonstrated promising results in distinguishing MSA from other neurodegenerative diseases (31). By in vitro autoradiography, the K_d values of [3 H]ACI-12589 was estimated to be 17 nM using brain tissues from a familiar PD and 28 nM using brain tissues from a MSA case. High-resolution autoradiography revealed radioactive accumulation on individual α -synuclein inclusions, aligning with the pathologies identified through immunohistochemical staining. Using AD tissues with $A\beta$ and tau aggregates, [3H]ACI-12589 showed a K_d value of 300 nM and a low maximal binding capacity, indicating its excellent specificity towards α -synuclein pathologies. In the preliminary clinical studies, compared to patients with PD, DLB, and healthy controls, participants diagnosed with MSA exhibited a greater retention of [18F]ACI-12589 in the cerebellar white matter, particularly in the phenotype dominated by parkinsonism (MSA-P) rather than in the phenotype dominated by cerebellar ataxia (MSA-C). The low density of α -synuclein pathologies, along with the variations in conformation and posttranslational modifications across different synucleinopathies, may explain the lack of specific accumulation in PD and DLB. Impressively, the study further included participants with progressive supranuclear palsy (PSP, three cases), hereditary ataxias (two cases), and AD (five cases). The radioactivity accumulation of [18F]ACI-12589 exhibited overlaps with pathologies identified by the tau tracer [18F]R0948, but showed a weak correlation with the positive regions observed by the A β PET tracer [18 F]flutemetamol. Similarly, the retention of [18F]ACI-12589 in PSP matched the expected tau pathology. This may be clarified by the co-pathologies of α -synuclein in AD and PSP. Further characterizations of the tracer's binding sites in various neurodegenerative diseases, along with an in-depth clinical investigation involving larger patient cohorts, would provide an answer.

Immense efforts have been devoted to developing α -synuclein PET tracers with enhanced selectivity. Mach et al. introduced heterocyclic moieties, such as diazaspirocyclic or bridged amino cores, to replace the piperazine in the nonselective lead compound (32). The key structureaffinity relationship is illustrated in Figure 3A. In comparison to compound 40, linking the 4-methoxy-N-phenylbenzamide and pyridine with either 2,8-diazaspiro[4.5]decane (4f), 1,4-diazepane (4m), or 3,8diazabicyclo[3.2.1]octane (4i and 4p) enhanced the selectivity of the structures toward α -synuclein. [11C]4i was subsequently obtained with high molar activity (106 \pm 56 GBq/ μ mol) and peaked brain uptake in nonhuman primates with SUV values of 1.68 \pm 0.54 at 4 min postinjection. In vitro binding assays using [3H]4i suggest an off-target to 4R tau, which may limit the application of [11C]4i in certain circumstances. [3H]asyn-44, featuring a pyridothiophene core structure, was reported by Neil et al. to have a potent K_i value of 1.85 nM using PD homogenates (Figure 3B, left) (33). In in vitro autoradiography studies, it generated a distinct radioactive signal in brain sections from MSA and PD, aligning with neuropathology visualized through anti-pS129 α -synuclein immunohistochemistry. The corresponding PET tracer [18F]asyn-44 was hindered by the penetrance of radiometabolite in the brain, preventing further evaluations. Imidazo[2,1-b][1,3,4]thiadiazole derivatives were proposed by Cui et al. as a novel scaffold, and [18F]FITA-2 was screened out with moderate affinity (IC $_{50,\,\alpha\text{-synuclein}} = 245$ nM, Figure 3B, right) (34). It possessed suitable brain uptake with sufficient clearance and good stability in healthy SD rats and is currently being evaluated in patients. Other chemical structures that may fulfill α -synuclein neuroimaging are discussed in recent reviews (35, 36).

In summary, extensive posttranslational modifications in vivo, including phosphorylation, truncation, and acetylation, may lead to changes in aggregation characteristics, such as structure and properties within the binding pocket. This results in varying binding potency of the structures to synthetic $\alpha\text{-synuclein}$ aggregates and human tissues. It seems to be an unavoidable trend to include brain sections or homogenates from donors with neurodegenerative conditions for compound screening. Binding assays of this kind include also the inherently low density of synucleinopathies. Molecular docking and photoaffinity labeling, alongside cryo-electron microscopy techniques, may assist in identifying



potential binding sites and optimizing structure (32, 37). Second, α -synucleinopathies are often accompanied by A β and tau aggregations that share a similar β -sheet structure, making it important and somewhat challenging to achieve selectivity. Recently, immunomagnetic cell sorting following in vivo radiotracer injection dissected the cellular allocation of 18-kDa translocator protein (TSPO)-PET signals in human glioma samples (38). We speculate that this approach may serve as a valuable tool to untangle the sources of radioactive signals in vivo from newly established α -synuclein PET tracers. In addition to the points mentioned above, the development of α -synuclein PET tracers encounters the typical challenges faced by molecular probes for central nervous system. It is essential to ensure sufficient molar activity, adequate brain penetration and to avoid confounding signals from radiometabolites in the brain (39). Nonetheless, the first promising clinical results have been disclosed. We believe that continuous scientific contributions from multiple disciplines will eventually pave the way for the development of α -synuclein PET tracers to illuminate synucleinopathies during disease progression.

Acknowledgments

A special thanks to Dr. Xiaoqing Song (Shanghai United Imaging Health-care Advanced Technology Research Institute) for constructive scientific interactions.

Author Contributions

Y.H. and L.Q. performed the literature review and wrote the original draft. Q.Y. and X.F. participated in reviewing and editing the manuscript. The manuscript has been read and approved by all authors. No related work is under consideration elsewhere.

Funding Sources

This publication was supported by STI2030-Major Projects (2022ZD0213800) and Shanghai Pujiang Program (23PJ1401500).

Author Disclosures

The authors have confirmed that no conflict of interest exists.

References

- 1. Tong J, Wong H, Guttman M, Ang LC, Forno LS, Shimadzu M, et al. Brain α -synuclein accumulation in multiple system atrophy, Parkinson's disease and progressive supranuclear palsy: a comparative investigation. Brain. 2010;133:172–88. DOI: 10.1093/brain/awp282. PMID: 19903734
- Spillantini GM, Schmidt ML, Lee VM-Y, Trojanowski JQ, Jakes R, Goedert M. Î-synuclein in Lewy bodies endogenous proviruses as "mementos"? Nature. 1997:839–40. DOI: 10.1038/42166. PMID: 9278044
- Goedert M, Spillantini MG, Del Tredici K, Braak H. 100 years of Lewy pathology. Nat Rev Neurol. 2013;9:13–24. DOI: 10.1038/nrneurol.2012.242. PMID: 23183883
- Brettschneider J, Irwin DJ, Boluda S, Byrne MD, Fang L, Lee EB, et al. Progression of alpha-synuclein pathology in multiple system atrophy of the cerebellar type. Neuropathol Appl Neurobiol. 2017;43:315–29. DOI: 10.1111/nan.12362. PMID: 27716988: PMCID: PMC5362365
- 5. Fusco G, De Simone A, Gopinath T, Vostrikov V, Vendruscolo M, Dobson CM, et al. Direct observation of the three regions in α -synuclein that determine its membrane-bound behaviour. Nat Commun. 2014;5:1–8. DOI: 10.1038/ncomms4827. PMID: 24871041; PMCID: PMC4046108
- 6. Vamvaca K, Volles MJ, Lansbury PT. The first N-terminal amino acids of α -synuclein are essential for α -helical structure formation in vitro and membrane binding in yeast. J Mol Biol. 2009;389:413–24. DOI: 10.1016/j.jmb.2009.03.021. PMID: 19285989: PMCID: PMC2801807
- 7. Nielsen MS, Vorum H, Lindersson E, Jensen PH. Ca2+ binding to α -synuclein regulates ligand binding and oligomerization. J Biol Chem. 2001;276:22680–4. DOI: 10.1074/jbc.M101181200. PMID: 11312271
- 8. Polymeropoulos MH, Lavedan C, Leroy E, Ide SE, Dehejia A, Dutra A, et al. Mutation in the α -synuclein gene identified in families with Parkinson's disease. Science. 1997;276:2045–7. DOI: 10.1126/science.276.5321.2045. PMID: 9197268
- 9. Zarranz JJ, Alegre J, Gómez-Esteban JC, Lezcano E, Ros R, Ampuero I, et al. The new mutation, E46K, of α -synuclein causes Parkinson and Lewy body dementia. Ann Neurol. 2004;55:164–73. DOI: 10.1002/ana.10795. PMID: 14755719
- Kiely AP, Asi YT, Kara E, Limousin P, Ling H, Lewis P, et al. A-synucleinopathy associated with G51D SNCA mutation: a link between Parkinson's disease and multiple system atrophy? Acta Neuropathol. 2013;125:753–69. DOI: 10.1007/ s00401-013-1096-7. PMID: 23404372; PMCID: PMC3681325
- 11. Kapasi A, Brosch JR, Nudelman KN, Agrawal S, Foroud TM, Schneider JA. A novel SNCA E83Q mutation in a case of dementia with Lewy bodies and

- atypical frontotemporal lobar degeneration. Neuropathology. 2020;40:620-6. DOI: 10.1111/neup.12687. PMID: 32786148; PMCID: PMC7787029
- 12. Diaw SH, Borsche M, Streubel-Gallasch L, Dulovic-Mahlow M, Hermes J, Lenz I, et al. Characterization of the pathogenic α -synuclein variant V15A in Parkinson's disease. NPJ Parkinsons Dis. 2023;9:148. DOI: 10.1038/s41531-023-00584-z. PMID: 37903765; PMCID: PMC10616187
- 13. Vekrellis K, Emmanouilidou E, Xilouri M, Stefanis L. α -synuclein in Parkinson's disease: 12 years later. Cold Spring Harb Perspect Med. 2024;14(11):a041645. DOI: 10.1101/cshperspect.a041645. PMID: 39349314; PMCID: PMC11529858
- Lee RMQ, Koh T-W. Genetic modifiers of synucleinopathies—lessons from experimental models. Oxford Open Neurosci. 2023;2:1–30. DOI: 10.1093/oons/kvad001. PMID: 38596238; PMCID: PMC10913850
- Kobylecki C, Langheinrich T, Hinz R, Vardy ERLC, Brown G, Martino ME, et al. 18F-florbetapir PET in patients with frontotemporal dementia and Alzheimer disease. J Nucl Med. 2015;56:386–91. DOI: 10.2967/jnumed.114.147454. PMID: 25655625
- 16. Li J, Huang Q, Qi N, He K, Li S, Huang L, et al. The associations between synaptic density and "A/T/N" biomarkers in Alzheimer's disease: an 18F-SynVesT-1 PET/MR study. J Cereb Blood Flow Metab. 2024;44:1199–207. DOI: 10.1177/0271678X241230733. PMID: 38295871; PMCID: PMC11179616
- Wu J, Li B, Wang J, Huang Q, Chen X, You Z, et al. Plasma glial fibrillary acid protein and phosphorated tau 181 association with presynaptic density-dependent tau pathology at 18F-SynVesT-1 brain PET imaging. Radiology. 2024;313:e233019. DOI: 10.1148/radiol.233019. PMID: 39560478; PMCID: PMC11605102
- 18. Fodero-Tavoletti MT, Mulligan RS, Okamura N, Furumoto S, Rowe CC, Kudo Y, et al. In vitro characterisation of BF227 binding to α -synuclein/Lewy bodies. Eur J Pharmacol. 2009;617:54–8. DOI: 10.1016/j.ejphar.2009.06.042. PMID: 19576880
- Bagchi DP, Yu L, Perlmutter JS, Xu J, Mach RH, Tu Z, et al. Binding of the radioligand SIL23 to α-synuclein fibrils in Parkinson disease brain tissue establishes feasibility and screening approaches for developing a parkinson disease imaging agent. PLoS One. 2013;8(2):e55031. DOI: 10.1371/journal.pone.0055031. PMID: 23405108; PMCID: PMC3566091
- 20. Chu W, Zhou D, Gaba V, Liu J, Li S, Peng X, et al. Design, synthesis, and characterization of 3-(Benzylidene)indolin-2-one derivatives as ligands for α -synuclein fibrils. J Med Chem. 2015;58:6002–17. DOI: 10.1021/acs.jmedchem.5b00571. PMID: 26177091; PMCID: PMC4624220
- 21. Maurer A, Leonov A, Ryazanov S, Herfert K, Kuebler L, Buss S, et al. 11 C-radiolabeling of anle253b: a putative PET tracer for Parkinson's disease that binds to α -synuclein fibrils in vitro and crosses the blood-brain barrier. ChemMedChem. 2020;15:411–5. DOI: 10.1002/cmdc.201900689. PMID: 31859430; PMCID: PMC7079211
- 22. Kuebler L, Buss S, Leonov A, Ryazanov S, Schmidt F, Maurer A, et al. [11 C]MODAG-001-towards a PET tracer targeting α -synuclein aggregates. Eur J Nucl Med Mol Imaging. 2021;48:1759–72. DOI: 10.1007/s00259-020-05133-x. PMID: 33369690; PMCID: PMC8113290
- 23. Bonanno F, Saw RS, Bleher D, Papadopoulos I, Bowden GD, Bjerregaard-andersen K, et al. Advancing Parkinson's disease diagnostics: the potential of Arylpyrazolethiazole derivatives for imaging α -synuclein aggregates. ACS Omega. 2024;9(23):24774–88. DOI: 10.1021/acsomega.4c01301. PMID: 38882134; PMCID: PMC11170759
- Yousefi BH, Arzberger T, Wester HJ, Schwaiger M, Yakushev I, Weber W, et al. Translational study of a novel alpha-synuclein PET tracer designed for first-in-human investigating. Nuklearmedizin. 2019;58(2):113. DOI: 10.1055/s-0039-1683494
- 25. Chen L, Huang G-L, Lü M-H, Zhang Y-X, Xu J, Bai S-P. Amide derivatives of Gallic acid: design, synthesis and evaluation of inhibitory activities against in vitro α -synuclein aggregation. Bioorg Med Chem. 2020;28:115596. DOI: 10.1016/j.bmc. 2020.115596. PMID: 32631566
- 26. Meng X, Munishkina LA, Fink AL, Uversky VN. Molecular mechanisms underlying the flavonoid-induced inhibition of α -synuclein fibrillation. Biochemistry. 2009;48:8206–24. DOI: 10.1021/bi900506b. PMID: 19634918
- 27. Xiang J, Tao Y, Xia Y, Luo S, Zhao Q, Li B, et al. Development of an α -synuclein positron emission tomography tracer for imaging synucleinopathies. Cell. 2023;186:3350–67.e19. DOI: 10.1016/j.cell.2023.06.004. PMID: 37421950; PMCID: PMCI0527432
- 28. Di Nanni A, Saw RS, Battisti UM, Bowden GD, Boeckermann A, Bjerregaard-Andersen K, et al. A fluorescent probe as a lead compound for a selective α -synuclein PET tracer: development of a library of 2-styrylbenzothiazoles and biological evaluation of [18F]PFSB and [18F]MFSB. ACS Omega. 2023; 8:31450–67. DOI: 10.1021/acsomega.3c04292. PMID: 37663501; PMCID: PMC10468942
- 29. Matsuoka K, Ono M, Takado Y, Hirata K, Endo H, Ohfusa T, et al. High-contrast imaging of α -synuclein pathologies in living patients with multiple system



- atrophy. Mov Disord. 2022;37:2159–61. DOI: 10.1002/mds.29186. PMID: 36041211; PMCID: PMC9804399
- 30. Endo H, Ono M, Takado Y, Matsuoka K, Takahashi M, Tagai K, et al. Imaging α -synuclein pathologies in animal models and patients with Parkinson's and related diseases. Neuron. 2024;112:2540–57.e8. DOI: 10.1016/j.neuron.2024.05. 006. PMID: 38843838
- 31. Smith R, Capotosti F, Schain M, Ohlsson T, Vokali E, Molette J, et al. The α -synuclein PET tracer [18F] ACI-12589 distinguishes multiple system atrophy from other neurodegenerative diseases. Nat Commun. 2023;14:6750. DOI: 10. 1038/s41467-023-42305-3. PMID: 37891183; PMCID: PMC10611796
- Kim HY, Chia WK, Hsieh CJ, Guarino DS, Graham TJA, Lengyel-Zhand Z, et al. A novel brain PET radiotracer for imaging alpha synuclein fibrils in multiple system atrophy. J Med Chem. 2023;66:12185–202. DOI: 10.1021/acs.jmedchem. 3c00779. PMID: 37651366; PMCID: PMC10617560
- Pees A, Tong J, Birudaraju S, Munot YS, Liang SH, Guarino DS, et al. Development of pyridothiophene compounds for PET imaging of α-synuclein. Chem. 2024;30:1–14. DOI: 10.1002/chem.202303921. PMID: 38354298
- 34. Zeng Q, Zhang X, Li Y, Zhang Q, Dai J, Yan XX, et al. Discovery and evaluation of imidazo[2,1-b][1,3,4]thiadiazole derivatives as new candidates for α -synuclein PET imaging. J Med Chem. 2024;67:12695–710. DOI: 10.1021/acs.jmedchem. 4c00686. PMID: 39080985
- Korat Š, Bidesi NSR, Bonanno F, Di Nanni A, Hoàng ANN, Herfert K, et al. Alphasynuclein PET tracer development-an overview about current efforts. Pharmaceuticals. 2021;14(9):847. DOI: 10.3390/ph14090847. PMID: 34577548; PMCID: PMC8466155
- Mekala S, Wu Y, Li Y. Strategies of positron emission tomography (PET) tracer development for imaging of tau and α-synuclein in neurodegenerative disorders. RSC Med Chem. 2024. DOI: 10.1039/d4md00576g. PMID: 39678127; PMCID: PMC11638850
- 37. Zhang S, Xiang H, Tao Y, Li J, Zeng S, Xu Q, et al. Inhibitor development for α -synuclein fibril's disordered region to alleviate Parkinson's disease pathol-

- ogy. J Am Chem Soc. 2024;146(41):28282. DOI: 10.1021/jacs.4c08869. PMID: 39327912; PMCID: PMC11669093
- Bartos LM, Kirchleitner SV, Kolabas ZI, Quach S, Beck A, Lorenz J, et al. Deciphering sources of PET signals in the tumor microenvironment of glioblastoma at cellular resolution. Sci Adv. 2023;9:eadi8986. DOI: 10.1126/SCIADV.ADI8986. PMID: 37889970; PMCID: PMC10610915
- Matthews PM, Rabiner EA, Passchier J, Gunn RN. Positron emission tomography molecular imaging for drug development. Br J Clin Pharmacol. 2012;73:175–86. DOI: 10.1111/j.1365-2125.2011.04085.x. PMID: 21838787; PMCID: PMC3269576

Publisher's note: Genomic Press maintains a position of impartiality and neutrality regarding territorial assertions represented in published materials and affiliations of institutional nature. As such, we will use the affiliations provided by the authors, without editing them. Such use simply reflects what the authors submitted to us and it does not indicate that Genomic Press supports any type of territorial assertions.

Open Access. This article is licensed to Genomic Press under the Creative Commons Attribution 4.0 International Public License (CC BY

4.0). The license requires: (1) Attribution — Give appropriate credit (creator name, attribution parties, copyright/license/disclaimer notices, and material link), link to the license, and indicate changes made (including previous modifications) in any reasonable manner that does not suggest licensor endorsement. (2) No additional legal or technological restrictions beyond those in the license. Public domain materials and statutory exceptions are exempt. The license does not cover publicity, privacy, or moral rights that may restrict use. Third-party content follows the article's Creative Commons license unless stated otherwise. Uses exceeding license scope or statutory regulation require copyright holder permission. Full details: https://creativecommons.org/licenses/by/4.0/. License provided without warranties